Bioinorganic Chemistry

DOI: 10.1002/anie.201002719

Catalytic Hydrogen Evolution from Mononuclear Iron(II) Carbonyl Complexes as Minimal Functional Models of the [FeFe] Hydrogenase Active Site**

Sandeep Kaur-Ghumaan, Lennart Schwartz, Reiner Lomoth, Matthias Stein, and Sascha Ott**

In nature, the reversible interconversion of protons to molecular hydrogen is catalyzed by enzymes termed hydrogenases (H_2ases). The structure elucidation of the [FeFe] H_2ases by X-ray crystallography[1,2] has provided a detailed picture of their active sites (Scheme 1) and has inspired

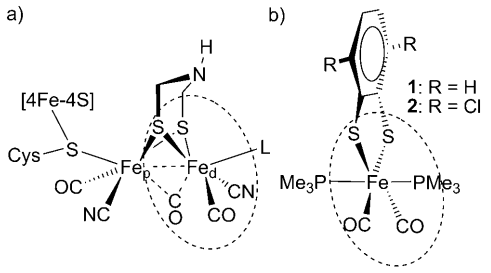

Scheme 1. a) The active site of the [FeFe] H_2ase and b) model complexes **1** and **2**. Structural similarities between Fe_d and **1** and **2** are highlighted.

bioinorganic chemists to search for model complexes that mimic the enzyme active site in structure and function.[3] Although the last ten years have seen intensive efforts and the preparation of more than 250 catalyst candidates,[4] difficulties remain to model functionally important features of the active site. First, Fe_2 complexes that are frequently used for electrocatalytic proton reduction usually involve the iron(0) oxidation state, which is different from the enzymatic process that exclusively employs iron(I) and iron(II) redox levels.[5,6] Second, the hydride that is an intermediate in the catalytic cycle of model complexes often resides in a bridging position between the two iron centers, unless special ligand sets are employed.[7,8] In contrast, nature uses terminal hydrides that are thermodynamically and kinetically more reactive. Third, a free or labile coordination site for substrate binding is crucial for enzyme activity,[9] but at the same time, a feature that is difficult to model owing to stability reasons.[10] Together, all the above points conspire to large overpotentials and low turnover rates that are frequently observed for catalysis by biomimetic models.

Although inspiration from [FeFe] H_2ases suggested the preparation of dimetallic systems in the past, DuBois and coworkers have recently shown that mononuclear nickel systems that mimic the dinuclear [NiFe] H_2ase active site are viable catalysts for hydrogen generation and activation.[11,12] A closer look at the [FeFe] H_2ase mode of action reveals that proton or hydrogen substrate binding and also the hydride–proton reaction exclusively occur at the iron distal to the [4Fe4S] cluster (Fe_d), suggesting that mononuclear iron complexes that mimic Fe_d may also be viable catalyst motifs.[13]

We have recently reported the synthesis of mononuclear Fe^{II} complexes **1** and **2**,[14] which contain structural features of the mononuclear [Fe] H_2ase active site,[15] but may as well be regarded as models of Fe_d in the [FeFe] H_2ase (Scheme 1). In analogy to Fe_d in the H_{ox} state, **1** and **2** are in a $+$II oxidation state. The Fe^{II} centers are ligated by a bidendate benzene-1,2-dithiolate (bdt), two *cis*-arranged CO ligands, and a PMe_3 ligand, which electronically resembles the cyanide ligand. A second PMe_3 completes the coordination sphere of **1** and **2**, which differ solely in the chloride substituents in **2**.

Herein, we demonstrate for the first time that mononuclear Fe^{II} complexes that mimic Fe_d of the [FeFe] H_2ase contain a number of appealing features that enable the compounds to catalyze the electrochemical reduction of protons. We present a mechanistic proposal for this process based on spectroscopic, electrochemical, and theoretical studies.

The IR spectra of complexes **1** and **2** each show two ν_{CO} absorptions at 2014, 1958 cm^{-1} and 2020, 1965 cm^{-1}, respectively.[16] It is interesting to note that **1**, **2** thus also show some spectroscopic resemblance to the mononuclear [Fe] H_2ase active site, which has ν_{CO} absorptions at 2011 and 1944 cm^{-1}.[17] The small difference between the absorptions of **1** and **2** are caused by the electron-withdrawing chloride

[*] Dr. S. Kaur-Ghumaan, Dr. L. Schwartz, Dr. R. Lomoth, Dr. S. Ott
Department of Photochemistry and Molecular Science
Uppsala University, Box 523, 75120 Uppsala (Sweden)
Fax: (+46) 18-471-6844
E-mail: reiner.lomoth@fotomol.uu.se
sascha.ott@fotomol.uu.se
Homepage: http://www.fotomol.uu.se
Dr. M. Stein[+]
Molecular and Cellular Modelling Group
Institute for Theoretical Studies
Schloss-Wolfsbrunnenweg 35, 69118 Heidelberg (Germany)
[+] Current address:
Max-Planck-Institut für Dynamik komplexer technischer Systeme
Sandtorstrasse 1, 39106 Magdeburg (Deutschland)

[**] Financial support from the Swedish Research Council (S.O.), the Wenner Gren Foundation (S. K.), the Swedish Energy Agency, the Knut and Alice Wallenberg Foundation, the Klaus Tschira Foundation (M.S.), and the EU (FP7 Energy 212508 "SOLAR-H2") is gratefully acknowledged.

Supporting information for this article is available on the WWW under http://dx.doi.org/10.1002/anie.201002719.

substituents in the latter. Addition of up to one equivalent of $HClO_4$ to solutions of **1** or **2** in CH_3CN results in small but noticeable shifts of the IR frequencies with conserved isosbestic points, as illustrated for complex **1** in Figure 1.

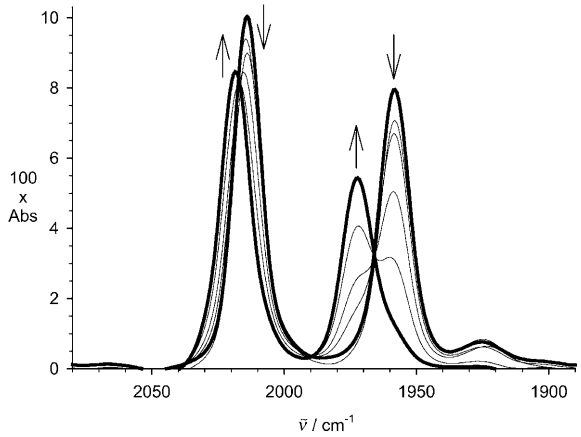

Figure 1. CO region in the IR spectrum of **1** (CH_3CN) in the presence of 0, 0.25, 0.5, 0.75, and 1 equiv of $HClO_4$.

Protonation is reversible, as demonstrated by the recovery of the original IR spectrum upon addition of pyridine. However, if more than three equivalents of $HClO_4$ are added, irreversible changes in the IR spectrum are observed and the compound decomposes. The pK_a of $\mathbf{2H}^+$ was estimated to be 11.5 by titration experiments with trifluoroacetic acid (TFA, pK_a = 12.5 in CH_3CN; see the Supporting Information).[18]

Complexes **1** and **2** are octahedral iron(II) complexes with a saturated coordination environment. Formation of a hydride species in analogy to a certain type of [FeFe] H_2ase active site models that form hydrides upon addition of strong acids[7] would require cleavage of a coordinative bond (see below). It is thus not surprising that ^{1}H NMR spectra of $\mathbf{1H}^+$ and $\mathbf{2H}^+$ show no signal in the hydride region. Instead, a splitting of the virtual triplet[19] from the PMe_3 protons in **1** and **2** into two doublets at different chemical shifts is observed. The aromatic protons in **1** experience an upfield shift and show an additional coupling; however, they remain the only signals in the aromatic region (Figure 2). ^{31}P NMR spectra of $\mathbf{1H}^+$ and $\mathbf{2H}^+$ feature two signals at $\delta = 0.8$, -2.4 ppm and $\delta = 0.0$, -3.1 ppm, respectively, compared to only one signal for **1** and **2** (see the Supporting Information). The NMR data thus suggest that protonation of the coordinatively saturated compounds **1** and **2** occurs at the sulfide of the bdt ligand and that the *S*-bound proton rapidly exchanges between the two sulfur centers on the NMR timescale. Bdt protonation has previously been described for $[Fe^{II}(bdt)_2]^{2-}$[20] and $[Fe_2(bpt)(CO)_4(Ph_2P(CH_2)_3PPh_2)]$.[21] DFT calculations yield structural parameters of **1** that are in good agreement with the crystal structure.[22] The calculations further support the assignment of the monoprotonated species, as the proton affinity of the bdt sulfur atom is 231 kcal mol^{-1} in the gas phase (B3LYP/TZVP) and 265 kcal mol^{-1} in CH_3CN, and thus larger than in all other calculated

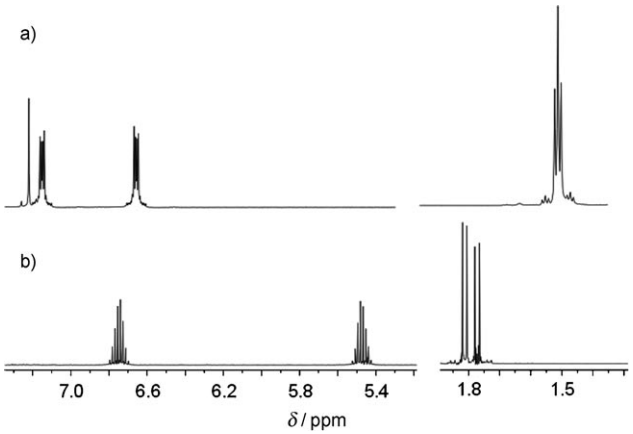

Figure 2. ^{1}H NMR spectra of **1** in CD_3CN at 298 K, a) without acid and b) with 1 equiv $HClO_4$.

monoprotonated species, such as a formyl ion (see the Supporting Information).

Electrochemically, **1** and **2** undergo reversible one-electron oxidations, at $E_{1/2} = 0.06$ and 0.10 V versus $Fc^{+/0}$, respectively, that are assigned to the $Fe^{II/III}$ couple. The 40 mV shift can be attributed to the chloride substituents in **2**, and the same trend can be seen for the reductions with cathodic peak potentials of $E_{pc} = -2.15$ and -2.34 V for **2** compared to -2.21 and -2.45 V for **1**. The reductions, presumably generating Fe^I and Fe^0 species, are irreversible, and the oxidation of unidentified products can be detected in the return scan (Figure 3a and the Supporting Information).

Upon addition of TFA to a solution of **2** in CH_3CN, two new reduction waves emerge at $E_{pc} = -1.2$ and -1.7 V.[23] Increasing the amount of added acid leads to an increase of the currents in both waves (Figure 3a). The background currents from the direct reduction of protons at the glassy carbon electrode are negligible at these potentials (see Supporting Information) and the acid-induced currents at -1.2 and -1.7 V can thus be attributed to catalytic turnover. Controlled potential electrolysis in combination with GC analysis provides further evidence for catalytic hydrogen production at the potential of both reduction peaks (Figure 3b). The decrease in catalytic activity during electrolysis is approximately paralleled by the depletion of **2** that was monitored by IR spectroscopy of the catholyte (ca. 25% reduction of the carbonyl bands from $\mathbf{2H}^+$ after 10 turnovers at -1.7 V).

The observation of two catalytic peaks with distinct turnover rates indicates that formation of H_2 from the same acid can proceed via two pathways that involve different oxidation states of the catalyst and are controlled by different rate-limiting steps (see also Scheme 2). The mechanism operating at the potential of the first wave could be rationalized by a CECEC sequence of chemical end electrochemical steps, in which protonation of the monoprotonated and monoreduced **2H** allows for further reduction at a similar potential. If this second protonation step occurs at the metal center, subsequent reduction will lead to a hydride species **2HHy** from which H_2 may be generated in a proton–hydride reaction. The more pronounced catalytic peak at -1.7 V is

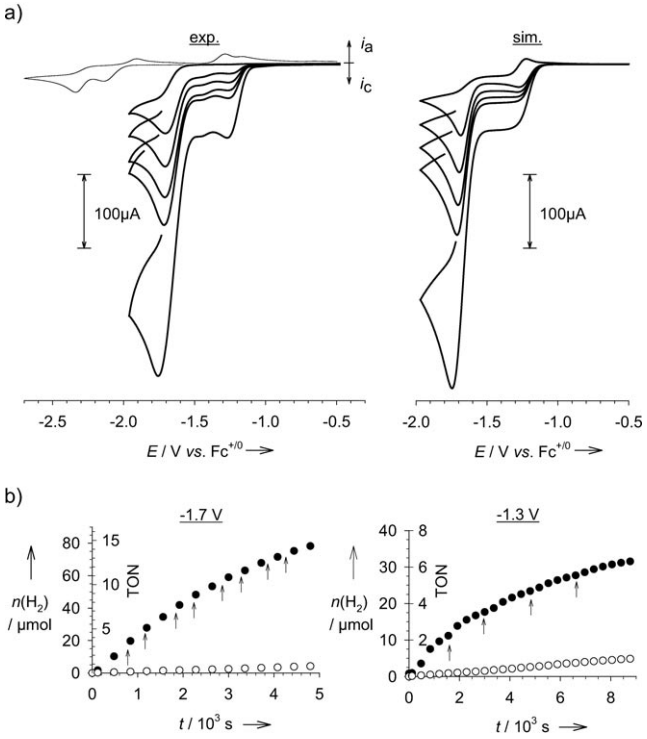

Figure 3. a) Cyclic voltammograms (0.1 Vs^{-1}) of **2** (1.5 mM) in the absence (thin curve) and presence (thick curves) of increasing TFA concentrations (9, 15, 21, 27, 66 mM) in CH_3CN with $[N(n\text{-}C_4H_9)_4][PF_6]$ (0.1 M). Reverse scans partly truncated for clarity. Simulated cyclic voltammograms of **2** in the presence of TFA (concentrations as above) and with the parameters specified in Scheme 2. b) Gas chromatographic quantification of H_2 and turnover number during controlled potential electrolysis of 5 mL 10 mM TFA with **2** (1.1 mM for −1.7 V, 1.0 mM for −1.3 V; ●) and background for direct hydrogen formation at the glassy carbon electrode (○). Arrows indicate addition of TFA to replace consumed acid.

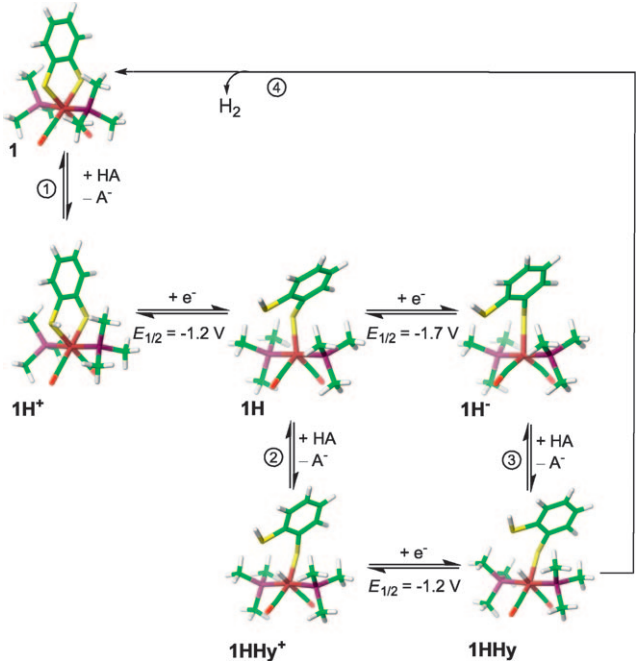

Scheme 2. Mechanistic proposal for the catalytic formation of hydrogen from the acid HA with DFT-optimized structures of proposed intermediates.[23,24] Parameters estimated from cyclic voltammetry data of complex **2** in the presence of TFA (Figure 3): $K_1 = 10^{-1}$, $k_1 = 2\times10^4$ $M^{-1}s^{-1}$; $K_2 \geq 10^{-1}$, $k_2 = 5\times10^1$ $M^{-1}s^{-1}$; $K_3 \geq 3\times10^7$ (thermodynamically superfluous), $k_3 \geq 10^5$ $M^{-1}s^{-1}$; $K_4 \geq 10^1$ M, $k_4 \geq 10^3$ s^{-1}.[23]

instead attributed to a CEECC mechanism that involves formation of the doubly reduced $\mathbf{2H}^-$ intermediate at the more negative potential. With the first and final steps being common to both mechanisms, the higher turnover frequency at −1.7 V can be attributed to the hydride formation step that would be expected to be favored at the iron(0) center of the $\mathbf{2H}^-$ intermediate.

Digital simulations (Figure 3a) based on the proposed mechanisms result in good agreement with the experimental voltammograms and provide estimates of the order of magnitude of the kinetic and thermodynamic parameters (Scheme 2). In terms of rate-limiting steps, the simulations indicate that the faster cycle operating at −1.7 V is limited by formation of $\mathbf{2H}^+$ (1) whilst the turnover rate at −1.2 V is restricted by the even slower formation of $\mathbf{2HHy}^+$ (2; see the Supporting Information for details). Catalysis at −1.2 V can be accelerated by replacing TFA with a stronger acid ($HClO_4$, $pK_a = 2$), an experiment which is, however, impeded by the limited stability of **2** with more than a slight excess of $HClO_4$ (see the Supporting Information). Overall, **2** is a more suitable catalyst for hydrogen formation from the weaker acid TFA with an overpotential of 0.3 V ($E^0_{TFA} = -0.87$ V) as compared to 0.9 V for $HClO_4$ ($E^0_{HClO_4} = -0.26$ V).[25] The faster turnover at −1.7 V requires lower limits on the order of 10^5 $M^{-1}s^{-1}$ for the formation of **2HHy** via $\mathbf{2H}^-$ (3) and on the order of 10^3 s^{-1} for the final step of H_2 formation and release (4).

Further support for the proposed mechanism was obtained from computational results on **1** that yielded information on the geometric and electronic structure of the intermediates that should apply analogously to **2**.[23,26,27] The redox potentials were directly computed relative to the one-electron reduction of $Fc^{+/0}$.[28,29] For the $\mathbf{1H}^+$**/1H** couple, the computed reduction potential (BP86/TZVP) of −0.9 V versus $Fc^{+/0}$ agrees well with the measured value and shows the suitability of the basis set.[30] Furthermore, the calculations show that the reduction of $\mathbf{1H}^+$ to **1H** is a combination of a metal- and ligand-orbital based reduction that results in cleavage of one Fe–S bond (Fe···SH distance in **1H** 4.20 Å compared to that of the intact Fe–S bond of 2.31 Å). The reductive cleavage of one iron–bdt bond leaves the Fe^I center in a five-coordinate environment. The free coordination site and sufficient electron density at Fe^I are necessary prerequisites for the second protonation of **1H**, which occurs at the Fe^I center and results in the formation of a formal hydride species $\mathbf{1HHy}^+$. Upon binding of the second proton to form $\mathbf{1HHy}^+$, atomic charges of the sulfur atoms display the largest changes, which indicates a re-orientation of the charge distribution in the complex (see the Supporting Information). The second metal-centered reduction at −1.2 V to form **1HHy** is followed by a re-orientation of the Fe–SH^+ bond to a geometry in which the S-bound proton could approach the

metal hydride, allowing for heterolytic H_2 formation. The Fe–$H^{-}\cdots{}^{+}$H–S distance changes from 3.98 Å in **1HHy** to 2.23 Å in the rotated form from which H_2 release is thermodynamically possible.

The computational results also corroborate the assignment of the more pronounced catalytic peak at −1.7 V to a CEECC mechanism. DFT calculations predict that the reduction from a formal Fe^{I} to a formal Fe^{0} occurs at −1.6 V versus $Fc^{+/0}$, that is, at 0.7 V more negative potential than the Fe^{II}/Fe^{I} couple. The second electron uptake is accompanied by a decrease in Fe···SH distance from 4.2 Å to 3.9 Å, which, in addition to the higher electron density, facilitates the proton–hydride reaction at the metal site and H_2 formation. The final step of H_2 release from **1HHy**, which is common to both mechanisms, was also supported by DFT results that predict the reaction to be exothermic by $\Delta G < -23\ \mathrm{kcal\,mol^{-1}}$.

In summary, we have shown for the first time that mononuclear ferrous complexes that mimic Fe_d of the [FeFe] H_2ase active site are capable of catalyzing the electrochemical reduction of protons. Among the two mechanistic pathways featured by the Fe^{II} complexes, the catalytic cycle operating with less overpotential omits any Fe^{0} intermediate that is often encountered in dinuclear model systems. As a consequence, the observed overpotential of 300 mV is less than that found for the majority of all conventional dinuclear complexes that have been reported as functional models of the [FeFe] H_2ase active site to date.[4] The oxidative addition of a proton to form the hydride intermediates (**1HHy**$^{+}$, **2HHy**$^{+}$) at the iron(I) level is enabled by the structural changes that occur upon the first reduction of **1H**$^{+}$ or **2H**$^{+}$; that is, the creation of an open binding site on the five-coordinate intermediates **1H** or **2H**. Under the conditions of this study (acid HA = TFA, [HA] < 100 mM), the bimolecular hydride formation remains however the rate-limiting step, and catalytic turnover is not restricted by the reactivity of the hydrides that are potentially more reactive than the bridging hydrides typically formed on dinuclear complexes. Further in-depth mechanistic studies, attempts to improve the stability of the complexes, and a study of an effect of changes in the second coordination sphere of the complexes are at the heart of ongoing work.

Received: May 5, 2010
Revised: July 6, 2010
Published online: September 15, 2010

Keywords: bioinorganic chemistry · enzyme catalysis · hydrogen production · hydrogenases · iron complexes

[1] J. W. Peters, W. N. Lanzilotta, B. J. Lemon, L. C. Seefeldt, *Science* **1998**, *282*, 1853 – 1858.
[2] Y. Nicolet, C. Piras, P. Legrand, E. C. Hatchikian, J. C. Fontecilla-Camps, *Structure* **1999**, *7*, 13 – 23.
[3] C. Tard, C. J. Pickett, *Chem. Rev.* **2009**, *109*, 2245 – 2274.
[4] G. A. N. Felton, C. A. Mebi, B. J. Petro, A. K. Vannucci, D. H. Evans, R. S. Glass, D. L. Lichtenberger, *J. Organomet. Chem.* **2009**, *694*, 2681 – 2699.
[5] P. E. M. Siegbahn, J. W. Tye, M. B. Hall, *Chem. Rev.* **2007**, *107*, 4414 – 4435.
[6] M. H. Cheah, C. Tard, S. J. Borg, X. Liu, S. K. Ibrahim, C. J. Pickett, S. P. Best, *J. Am. Chem. Soc.* **2007**, *129*, 11085 – 11092.
[7] F. Gloaguen, T. B. Rauchfuss, *Chem. Soc. Rev.* **2009**, *38*, 100 – 108.
[8] B. E. Barton, T. B. Rauchfuss, *Inorg. Chem.* **2008**, *47*, 2261 – 2263.
[9] F. A. Armstrong, *Curr. Opin. Chem. Biol.* **2004**, *8*, 133 – 140.
[10] L. Schwartz, J. Ekström, R. Lomoth, S. Ott, *Chem. Commun.* **2006**, 4206 – 4208.
[11] A. D. Wilson, R. K. Shoemaker, A. Miedaner, J. T. Muckerman, D. L. DuBois, M. R. DuBois, *Proc. Natl. Acad. Sci. USA* **2007**, *104*, 6951 – 6956.
[12] M. R. DuBois, D. L. DuBois, *Chem. Soc. Rev.* **2009**, *38*, 62 – 72.
[13] C. Mealli, T. B. Rauchfuss, *Angew. Chem.* **2007**, *119*, 9100 – 9102; *Angew. Chem. Int. Ed.* **2007**, *46*, 8942 – 8944.
[14] L. Schwartz, P. S. Singh, L. Eriksson, R. Lomoth, S. Ott, *C. R. Chim.* **2008**, *11*, 875 – 889.
[15] T. Hiromoto, K. Ataka, O. Pilak, S. Vogt, M. S. Stagni, W. Meyer-Klaucke, E. Warkentin, R. K. Thauer, S. Shima, U. Ermler, *FEBS Lett.* **2009**, *583*, 585 – 590.
[16] The broad absorption at 1925 $\mathrm{cm^{-1}}$ is attributed to an isomer.
[17] E. J. Lyon, S. Shima, R. Boecher, R. K. Thauer, F.-W. Grevels, E. Bill, W. Roseboom, S. P. J. Albracht, *J. Am. Chem. Soc.* **2004**, *126*, 14239 – 14248.
[18] Due to the milder reduction potential of **2** compared to **1**, only the former will be discussed in some instances, although all statements also hold qualitatively for **1**.
[19] R. K. Harris, *Can. J. Chem.* **1964**, *42*, 2275 – 2281.
[20] D. Sellmann, M. Geck, M. Moll, *J. Am. Chem. Soc.* **1991**, *113*, 5259 – 5264.
[21] S. Ezzaher, A. Gogoll, C. Bruhn, S. Ott, *Chem. Commun.* **2010**, *46*, 5575 – 5577.
[22] Our DFT results (BP86/TZVP) describe structural paramaters of **1** to within 0.04 Å of the crystal structure (see Ref. [14]), which is typical for this functional and basis set.[30]
[23] All electrocatalysis experiments were performed on complex **2**. To avoid complications with the chloride substituents, DFT calculation were performed on complex **1**. The mechanistic details are expected to be identical for both complexes.
[24] Intermediates **1H** and **1HHy**$^{+}$ are paramagnetic $S = {}^{1}/_{2}$ species. The predicted EPR parameters, such as g-tensor principal values and hyperfine coupling constants, can be found in the Supporting Information.
[25] G. A. N. Felton, R. S. Glass, D. L. Lichtenberger, D. H. Evans, *Inorg. Chem.* **2006**, *45*, 9181 – 9184.
[26] G. A. N. Felton, A. K. Vannucci, J. Chen, L. T. Lockett, N. Okumura, B. J. Petro, U. I. Zakai, D. H. Evans, R. S. Glass, D. L. Lichtenberger, *J. Am. Chem. Soc.* **2007**, *129*, 12521 – 12530.
[27] S. Canaguier, L. Vaccaro, V. Artero, R. Ostermann, J. Pécaut, M. J. Field, M. Fontecave, *Chem. Eur. J.* **2009**, *15*, 9350 – 9364.
[28] P. Surawatanawong, J. W. Tye, M. Y. Darensbourg, M. B. Hall, *Dalton Trans.* **2010**, *39*, 3093 – 3104.
[29] P. Surawatanawong, M. B. Hall, *Inorg. Chem.* **2010**, *49*, 5737 – 5747.
[30] C. Greco, G. Zampella, L. Bertini, M. Bruschi, P. Fantucci, L. D. Gioia, *Inorg. Chem.* **2007**, *46*, 108 – 116.

